Cell. Mol. Life Sci. (2012) 69:267–282
DOI 10.1007/s00018-011-0652-3

Cellular and Molecular Life Sciences

RESEARCH ARTICLE

The role of *LamininB2* (*LanB2*) during mesoderm differentiation in *Drosophila*

Georg Wolfstetter · Anne Holz

Received: 16 September 2010 / Revised: 2 February 2011 / Accepted: 15 February 2011 / Published online: 9 March 2011

Abstract In *Drosophila*, four genes encode for laminin subunits and the formation of two laminin heterotrimers has been postulated. We report the identification of mutations in the *Drosophila LamininB2* (*LanB2*) gene that encodes for the only laminin γ subunit and is found in both heterotrimers. We describe their effects on embryogenesis, in particular the differentiation of visceral tissues with respect to the ECM. Analysis of mesoderm endoderm interaction indicates disrupted basement membranes and defective endoderm migration, which finally interferes with visceral myotube stretching. Extracellular deposition of laminin is blocked due to the loss of the LanB2 subunit, resulting in an abnormal distribution of ECM components. Our data, concerning the different function of both trimers during organogenesis, suggest that these trimers might act in a cumulative way and probably at multiple steps during ECM assembly. We also observed genetic interactions with *kon-tiki* and *thrombospondin*, indicating a role for laminin during muscle attachment.

Keywords Myogenesis · Visceral mesoderm · Myoblast · Muscle attachment · Extracellular matrix · ECM · *kon-tiki* · *thrombospondin*

Introduction

The larval midgut of *Drosophila* consists of an inner endodermal gut tube and an outer visceral muscle layer formed by circular and longitudinal muscles. Visceral mesoderm formation starts independently from the endoderm with the segregation of 11 *bagpipe* (*bap*) and *binou* (*bin*)-expressing cell clusters along the inner germ band at stage 10 while the anlagen for the midgut endoderm are located anterior and posterior in two spatially separated primordia in the early embryo. At stage 11, the visceral cell clusters rearrange into visceral cell rows consisting of different myoblast subtypes while the endodermal primordia start to migrate towards the center of the embryo using the visceral mesoderm as a track. By stage 13, epithelial cells of the endoderm flank the central yolk, while the binucleate visceral syncytia expand dorsally and ventrally, organize themselves together with the longitudinal muscles as an interwoven web, and surround the midgut endoderm during a final elongation process. The visceral muscles subsequently start to constrict the midgut, which is finally subdivided into four chambers [1–11].

The role of the position-specific (PS) integrins during midgut migration and development has been intensively studied. It seems that PS2 integrin is required in the visceral mesoderm to provide the substratum for the midgut primordia migration, whereas the PS1 and PS3 integrins are essential in the endodermal cells for their movement along the visceral strands [12]. Integrins are heterodimeric, transmembrane receptors that act as primary cellular receptors for ECM molecules, such as laminin and collagen [13, 14]. Laminin is the most abundant cell adhesion molecule of basement membranes (BM) and is supposed to self-assemble into mesh-like networks that are connected via entactin/nidogen to the collagen network [15–17]. In *Drosophila*, four *Laminin* genes have been identified that encode for two α chains: a α3, 5 homolog referred to as lamininA (LanA) and a α1, 2 laminin encoded by the *wing blister* (*wb*) locus, one β (lamininB1, LanB1) and one γ

G. Wolfstetter · A. Holz (✉)
Institut für Allgemeine und Spezielle Zoologie,
Justus-Liebig-Universität Giessen, Stephanstrasse 24,
35390 Giessen, Germany
e-mail: anne.holz@allzool.bio.uni-giessen.de

subunit (lamininB2, LanB2), respectively. Together, these chains form two heterotrimeric proteins consisting of a LanB1/LanB2 core unit that associates either with LanA or Wb so that the diversity of *Drosophila* laminins is restricted to these two distinct $\alpha\beta\gamma$ trimers [18–20]. In contrast to this, studies on vertebrate laminins revealed the existence of several α, β, and γ chains that can be assembled combinatorial to form the native laminins [21]. In *Drosophila*, both laminin trimers are responsible for viability and the absence of each trimer due to separate null mutations in each α chain leads to embryonic phenotypes in somatic muscles, heart, and trachea morphogenesis, whereas adult phenotypes are associated with wing blistering and rhabdomere structure, suggesting an important role for structural organization and morphogenesis [18, 22–24]. Moreover, analysis of *LamininB1* (*LanB1*) mutations, resulting in complete loss of laminin function, revealed novel roles in basement membrane organization and therefore in cell adhesion and migration [25].

In this study, we examine the influence of the ECM on the process of visceral muscle and midgut differentiation by the analysis of newly identified *Drosophila LamininB2* (*LanB2*) mutations. We observed BM disruption and irregular initial stretching after myoblast fusion in the circular muscles of *LanB2* mutant embryos that also display a partially late myotube outgrowth and an elongation defect. The absence of endodermal epithelium formation in *LanB2* further suggests that an ECM-covered endodermal layer is necessary to achieve proper elongation and outgrowth of visceral muscles. Moreover, a weak muscle phenotype observed in *LanB2* mutant embryos was strongly enhanced in genetic interaction experiments with *kon-tiki* also known as *perdido* and *thrombospondin* uncovering new roles for laminin in muscle target site recognition and muscle attachment maintenance.

Materials and methods

Fly stocks and genetics

Flies were grown under standard conditions and crosses were performed at room temperature or at 25°C with the exception of RNAi crosses, which were performed at 29°C. Staging of embryos was done according to Campos-Ortega and Hartenstein [3]. The following mutations and fly stocks were used in this study: as *wild-type* (*wt*) stock we used $white^{1118}$ or balanced sibling embryos. *knödel* (*knod*) is one of two visceral mutations we discovered in the allele *3B1-038* of the EMS collection produced and described by Hummel et al. [26, 27]. We separated both mutations by meiotic recombination and established independent stocks for *knod* and the previously described second visceral mutation hkb^{gurt} [28]. Due to the identification of the mutation in *knödel* as *LamininB2* (*LanB2*) allele we refer to this allele as $LanB2^{knod}$ and to a second allele as $LanB2^{2}$ referred by Leicht and Bonner [29] as $l(3)67BDb^{1}$. A third *LanB2* allele $Mi\{ET1\}LanB2^{MB04039}$ was used for complementation tests. Other alleles used are *Df(2L)Exel7022* as deficiency for both type IV collagen genes (*viking* and *Cg25C*), *Df(3L)Exel6114* as *LanB2* deficiency, *Df(3L)Exel8101* and *Df(3L)BSC373* as deficiencies for *LamininA*, the null allele $LanA^{9-32}$ [22] and wb^{HG10} [30], wb^{SF25} [31] as well as *Df(2L)ED8186* and *Df(2L)ED793* as deficiencies for *Laminin wing blister*. As reporter lines, we used *hand-GFP* [32], *crocodile-lacZ* (*croc-lacZ*) [33] and vkg^{G454} [34]. *daughterless-GAL4* (*da-GAL4* also known as $GAL4^{daG32}$) [35], $P\{GawB\}CG5790^{NP1233}$ (Insertion that resembles the embryonic visceral *FasciclinIII* expression and is therefore referred to as *FasIII-GAL4*) (DGRC) as well as *UAS-LanB2RNAi* [36] and *P{UAS-Moesin::GFP}TC2* (referred to as *UMG*) [37] were used.

For genetic interaction experiments, we used $thrombospondin^{D77}$ (tsp^{D77}) [38] and the *kon-tiki* (*kon*) allele $kon\text{-}tiki^{NP7048}$ (kon^{NP7048}), and for further control experiments, we employed the deficiency *Df(2L)BSC149* (*kon* is also known as *perdido*) [39, 40]. For testing of genetic interaction, we removed one copy of *kon* (or *LanB2*) in homozygous *LanB2* (or *kon*) mutant embryos by crossing balanced heterozygous *kon* with *LanB2*. Double heterozygous offspring were crossed inter se and the stained offspring were compared with the stained progeny of crossings resulting from double heterozygous animals with flies of both parental (bearing the single heterozygous mutation) lines, respectively. Homozygous mutant *LanB2* embryos were distinguished by their changed nidogen distribution and their midgut morphology whereas homozygous mutant *kon* and *tsp* embryos can be recognized by their characteristic somatic muscle phenotype.

Immunofluorescent stainings, antibodies, and in situ hybridization

Embryos were fixed, immunostained, and prepared for in situ hybridization as described previously [41]. Fragments of *LamininA* and *LamininB2* were amplified from genomic DNA or the cDNA clone LD15803 (BDGP) with the following primer combinations: for *LanA* (GGTTCCGTGC TCTGAGCAGGTGGAA-GACAATAGCCCTGCCAAAT ATCGCCA) and for *LanB2* (GAGACTGGAATCTGCTT CTGCAAGGA-GAACCAAAGTAACCCTTCGGGCAC). TRITC-conjugated phalloidine (Sigma) was used for F-actin detection. We used the following primary antibodies: sheep anti-digoxygenin (1:1,000, Boehringer), rabbit anti-dystroglycan Dg^{ex8} (1:500) [42], rat anti-*Drosophila*-epithelial-cadherin (1:100, DSHB) [43], mouse

anti-fasciclin II (1:10, DSHB) [44], mouse anti-fasciclin III (1:10) [45], rat anti-filamin1/cheerio (1:500) [46], rabbit anti-β-galactosidase (1:2,500, Cappel), rabbit anti-green fluorescent protein (1:500, abcam), rabbit anti-lamininB2 (1:300, abcam), rabbit anti-laminin (1:500) [47], mouse anti-macrophage-derived-proteoglycan-1 (1:200) [48], rabbit anti-nidogen (1:5,000) [28], mouse anti-pericardin EC11 (1:5, DSHB) [49], rabbit anti-serpent (1:500, gift from Rolf Reuter), rabbit anti-SPARC (1:500) [50] and guinea-pig anti-β3tubulin (1:6,000) [51]. We used Cy2 and Cy3-conjugated secondary antibodies at 1:100 (Dianova), pre-absorbed biotinylated secondary antibodies at 1:500 in combination with the Vectastain ABC Kit Standard (Vector Laboratories) and the TSA Amplification Renaissance Kits (PerkinElmer). Embryos were embedded in Fluoromount-G (Southern Biotech) before visualization under a Leica TCS SP2 confocal microscope.

Results

Identification and characterization of *LamininB2* alleles

Recently, we reported the detection of a second site mutation on the EMS chromosome *3B1-038* that also carries the novel *huckebein* (*hkb*) allele hkb^{gurt} [26, 28]. This second site mutation caused dumpling-shaped midgut morphology in mutant embryos and was therefore named *knödel* (*knod*). The *knod* mutation was separated by meiotic recombination from the *3B1-038* chromosome. Complementation tests uncovered that *knod* maps to *Df(3L) Exel6114* which, among others, deletes the *LamininB2* (*LanB2*) locus (*Df LanB2*). Since transheterozygous animals display an abnormal midgut morphology, we analyzed all lethal mutations that fail to complement the deleted region in order to identify further *knod* alleles (Fig. 1). We identified $l(3)67Db^{1}$ a DEB-induced allele generated by Leicht and Bonner [29] and $LanB2^{MB04039}$, which carries a *Mi{ET1}* insertion in the 3′UTR of the *LanB2* gene as new *knod* alleles. DNA sequencing analysis of the *LanB2* gene in *knod* mutant embryos (further referred to as $LamininB2^{knödel}$, $LanB2^{knod}$) identified a C to T transition in *knod* that leads to a stop codon at position R948. We also detected an aberration in the coding sequence of the DEB-induced allele $l(3)67Db^{1}$ ($LamininB2^{2}$, $LanB2^{2}$) that induces a frame shift starting at position 2598. In consequence of this frame shift, E867 is changed to Alanine and a stop codon is induced at position C868. Concerning the structural properties of LanB2 [20], it is most likely that in both alleles *LanB2* encodes for truncated proteins that lack the C-terminal coiled-coil domain (Fig. 1a) which is pivotal for laminin trimer formation and secretion [52].

Further analyses of the *LanB2* alleles unveil that $LanB2^{MB04039}$ animals hatch and survive until larval stages (data not shown), while mutant embryos of $LanB2^{knod}$ and $LanB2^{2}$ die at the end of embryogenesis. This and further genetic analyses (Fig. 1) imply that $LanB2^{MB04039}$ is a weak loss-of-function (hypomorphic) allele while $LanB2^{knod}$ and $LanB2^{2}$ represent strong loss of function, probably amorphic alleles of *LamininB2*. This assumption is further supported since $LanB2^{knod}$, $LanB2^{2}$, and *Df LanB2* mutant embryos as well as transheterozygous animals (Fig. 1c–g) uniformly display the characteristic dumpling-shaped midgut and often exhibit local accumulations (Fig. 1g, arrowhead) and gaps (Fig. 1g, asterisk) in the visceral muscles. In accordance with earlier findings [24], we could not detect any difference in early visceral mesoderm formation (Fig. 1h, i), indicating that LanB2 might function during later steps of visceral muscle development. A potential maternal expression component could also mask early visceral mesoderm defects in *LanB2* mutant animals. However, this seems unlikely since an organized ECM around the visceral mesoderm is not present at this time (Fig. 2d) and no maternal component of *LanB2* had been detected by Northern-blot analyses [20].

LanB2 functions during organogenesis

Besides the examination of the characteristic visceral morphology (Figs. 1b–g, 3, 5) we focused our analyses of *LanB2* mutants on the embryonic development of other mesodermal-derived tissues. In *LanB2* mutant embryos, single muscles at random positions were not formed, leaving gaps in the somatic muscle pattern (Fig. 1k, asterisks) and single muscles display incomplete myoblast fusion (Fig. 1m, arrowheads). We also observed that the ventral oblique muscles in the four anterior segments were not attached to their tendon sites or were completely absent (arrows in Fig. 1o) resembling a common phenotype of *LanA*, *wing blister* and *LanB1* mutant embryos [18, 24, 25]. Since these analyses also revealed characteristic heart defects for *LanA, wb*, and *LanB1* we analyzed heart morphology in the absence of *LanB2*. At the end of embryogenesis, the heart consists of cardial and pericardial cells that can be labeled with *hand-GFP* and are covered with pericardin (PRC)-positive ECM (Fig. 1p). In *hand-GFP*; $LanB2^{knod}$ mutant embryos, the contact between pericardial cells and the heart tube is lost, resulting in the dissociation of pericardial cells. We also observed that pericardin is not localized properly at the basal surface of the cardial cells (Fig. 1q). Due to the strong expression of *LanB2* in the fat body (Fig. 2), we analyzed fat body differentiation of *wt* and *LanB2* mutant embryos double-stained with antibodies to serpent (SRP) [53] and FASIII. We could not detect any obvious changes upon stage 15, when fragmentation of fat body parts that

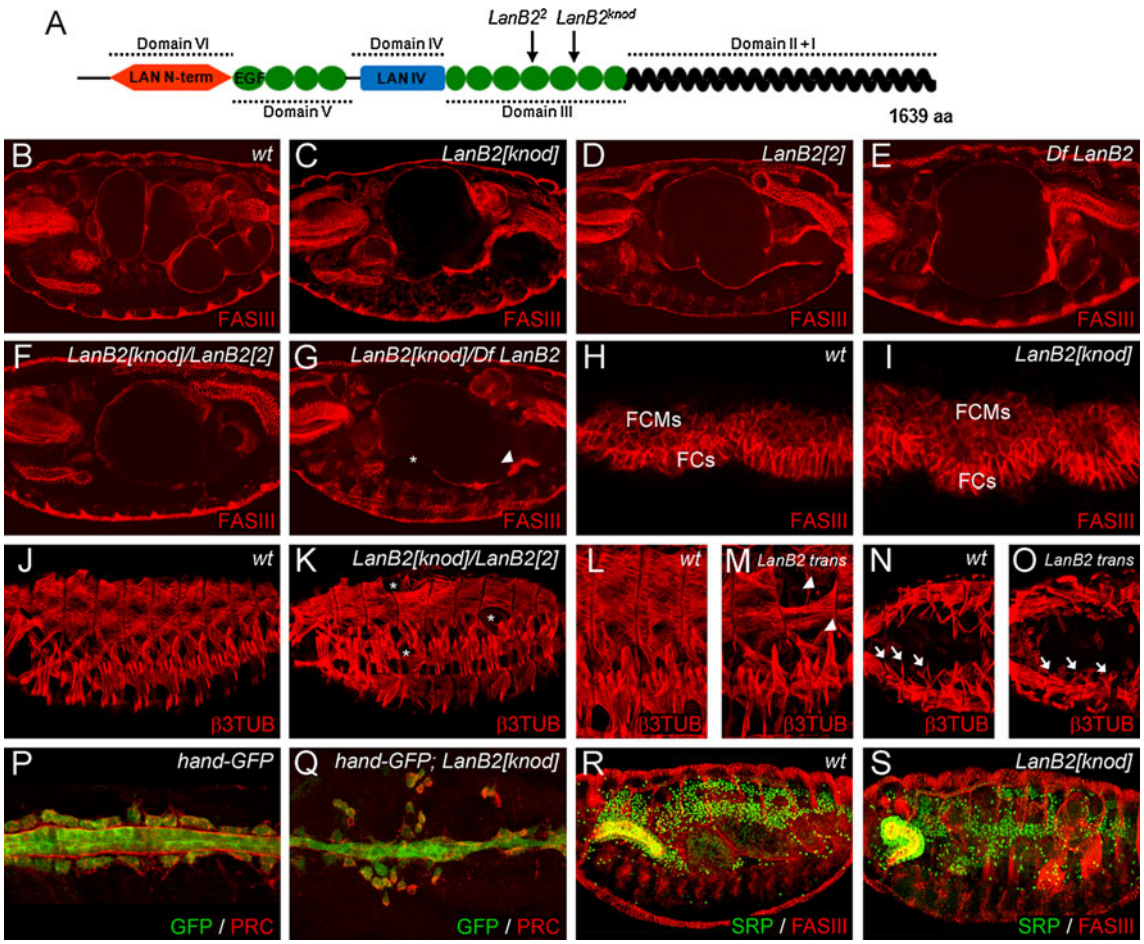

Fig. 1 The role of *LamininB2* (*LanB2*) during organogenesis. **a** Schematic representation of the lamininB2 subunit and the position of STOP codons induced in mutant alleles. At stage 16, a four-chambered midgut, surrounded by a thin sheet of FASIII-positive visceral muscles has formed in *wt* embryos (**b**). Mutant embryos of $LanB2^{knod}$ (**c**) and $LanB2^{2}$ (**d**) as well as *Df LanB2* (**e**) and transheterozygous $LanB2^{knod}/LanB2^{2}$ (**f**) and $LanB2^{knod}/Df\ LanB2$ (**g**) animals develop a one-chambered midgut and exhibit local accumulations (*arrowhead* in **g**) and gaps (*asterisk* in **g**) within the visceral muscle layer. No differences in early visceral mesoderm morphology and formation of visceral founder cells (*FCs*) and fusion competent myoblasts (*FCMs*) are visible between *wt* (**h**) and $LanB2^{knod}$ mutant (**i**) embryos. The segmental muscle pattern observed in *wt* embryos (**j**) is affected by randomly positioned gaps (*asterisks* in **k**) in $LanB2^{knod}/LanB2^{2}$. Single muscles are missing, unfused myoblasts (*arrowheads* in **m**) and not attached muscles are visible in $LanB2^{knod}/LanB2^{2}$ mutant embryos (*LanB2 trans*). Anterior, most located ventral oblique muscles (*arrows* in **n**) are missing (*arrows* in **m**) in *LanB2 trans* embryos (**o**). Pericardial cells flank the heart tube that is covered with pericardin (PRC)-positive ECM in stage 16 *hand-GFP*-expressing *wt* embryos (**p**). In $LanB2^{knod}$ animals (**q**), the pericardial cells detach from the heart tube and a proper localization of PRC fails. Compared to the *wt* situation (**r**), the fat body of late-stage $LanB2^{knod}$ mutant embryos (**s**) shows local disruptions and partially fails to attach to the tip of the incorrectly migrated salivary gland

neighbor the midgut becomes visible in *LanB2* mutant embryos (Fig. 1r, s). We also observed that the contact between fat body cells and the tip of the salivary gland is partially lost in *LanB2* mutant animals that also display defects during salivary gland turning and migration. In agreement with earlier observations made on *LanB1* and *wb* mutant embryos, *LanB2* animals display gaps in the dorsal trunk and the visceral branches of the trachea and show an altered migration and distribution of hemocytes as well as the improper condensation of the ventral nerve cord (data not shown). Taken together, *LanB2* seems to be involved in multiple steps of organ development which is resembled by the variety of phenotypes observed in *LanB2* mutant embryos. The fact that these phenotypes are in common with those reported for other laminin and integrin subunits, highlights the role of laminin as ligand during integrin-mediated morphogenesis.

Laminin expression and localization during embryogenesis

Since laminins act as secreted glycoproteins in the ECM, the deposition of the laminin trimers should differ from the tissue-specific expression of *Laminin* transcripts.

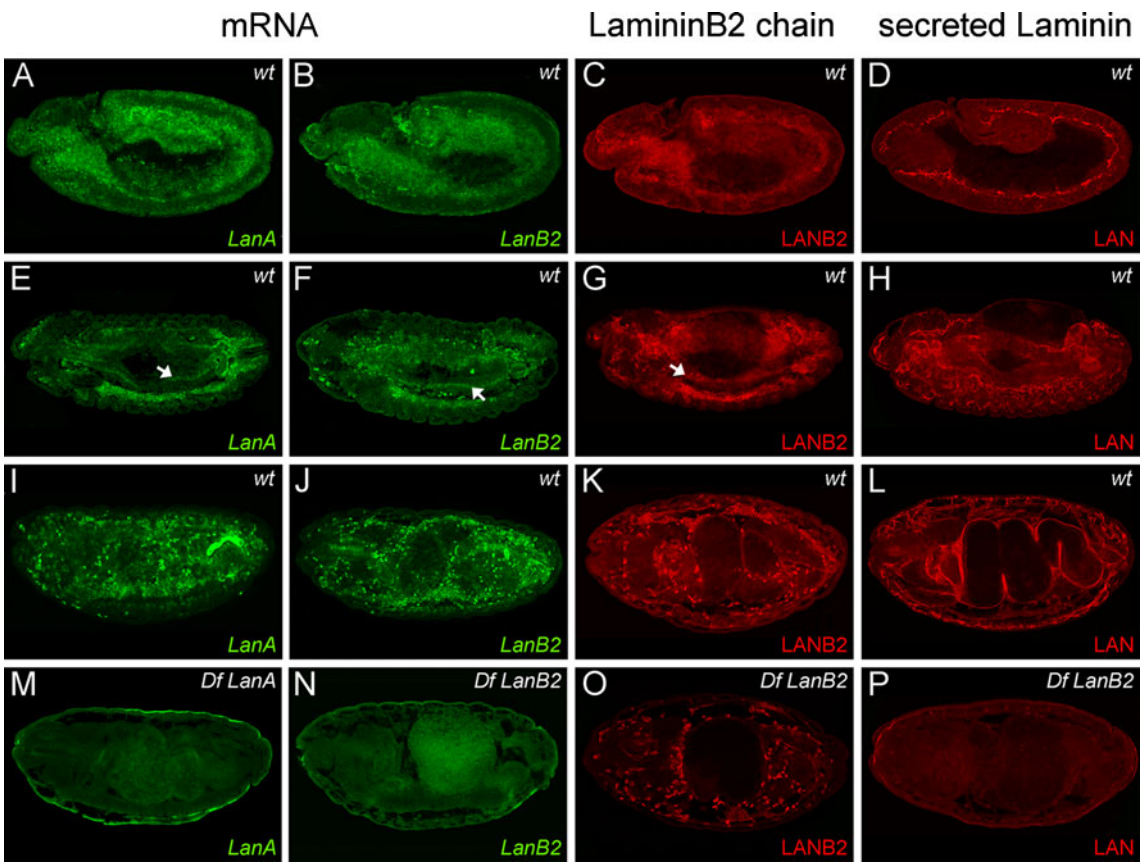

Fig. 2 Laminin expression and localization during embryogenesis. **a–d** At stage 11, transcripts of *LanA* and *LanB2* can be detected in the mesoderm and the midgut primordia that also express the LANB2 subunit, while extracellular LAN is found at the early basement membrane. **e–h** At stage 13, the mesodermal expression of *LanA, LanB2*, and the LANB2 protein is restricted to hemocytes, the fat body, and endodermal cells (*arrows* in **e–g**), while secreted LAN covers the surface of most internal organs. **i–k** At stage 15/16, *Laminin* transcripts and LANB2 expression remain most abundant in the fat body and the hemocytes. **l** At this time, LAN distribution is found around all internal organs and at the muscle tendon sites. **m–p** *Df LanA* and *Df LanB2* embryos do not show any specific staining of *Laminin* transcripts or secreted LAN. Intracellular signals of the LANB2 antibody are still present in hemocytes and fat body of *LanB2*-deficient embryos, indicating a potential cross reactivity with other, non-secreted laminin subunits

Therefore, we employed in situ hybridizations to *LanA* and *LanB2* transcripts. In *wt* embryos at stage 11, transcripts of *LanA* and *LanB2* (Fig. 2a, b) can be detected in mesodermal tissues along the germ band, the midgut primordia and the cephalic mesoderm that comprises the anlage for hemocytes [54]. *LanA* and *LanB2* expression increases in the fat body and hemocytes but decreases in the residual mesoderm (Fig. 2e, f) during germ band retraction. *Laminin* expression also concentrates in endodermal cells at the contact sites towards the outgrowing circular visceral muscles (Fig. 2e, f, arrows). During later stages, *Laminin* transcripts remain most prominent in mature hemocytes and the fat body (Fig. 2i, j). These results are in accordance with findings of Montell and Goodman [20] who reported a common expression pattern for *LanA*, *LanB1*, and *LanB2*. The expression of *LanA* and *LanB2* in appropriate deficient embryos shows complete loss of the respective expression patterns (Fig. 2m, n).

For analyzing the expression pattern of single laminin monomers and the extracellular deposition of laminin trimers, we used antibodies to the lamininB2 subunit [55] and antibodies specific for secreted laminin [47] trimers. Antibodies to lamininB2 (LANB2) label the mesoderm and both midgut primordia at stage 11 (Fig. 2c) and stage 13 embryos show staining in hemocytes, fat body, and the midgut endoderm (Fig. 2g, arrow). While *wt* embryos at stage 16 (Fig. 2k) display LANB2 expression in the fat body and hemocytes, staining of *LanB2*-deficient embryos (Fig. 2o) reveals that intracellular signals in hemocytes and fat body are still present. As antibodies to the LanB1 protein [55] produced the same staining pattern on *LanB2*-deficient embryos and vice versa (data not shown), we assumed that there might be cross reactivity between the remaining intracellular laminin subunits and the LANB2 antibody. Staining for secreted laminin trimers (LAN) displays strong signals in stage 11 *wt* embryos where

laminin is located at BMs that separates the neuroectoderm from mesodermal tissues (Fig. 2d). During later stages, extracellular laminin covers most internal organs like the midgut primordia, the visceral muscles, malpighian tubules, and the fat body (Fig. 2h). At the end of embryogenesis, high staining levels can be observed at the muscle tendon sites and BMs surrounding the brain, nerve cord and the gut (Fig. 2l). In contrast to the LANB2 antibody, we did not detect LAN staining in *LanB2*-deficient embryos (Fig. 2p) and *LanB2*^{knod} mutant embryos (Fig. 3h), reflecting the affinity of this antibody only for secreted laminins. Taken together, these results suggest that secretion and extracellular deposition of laminin trimers fail due to the loss of the LanB2 subunit.

Different *Laminin* trimers are involved in ECM assembly and midgut morphogenesis

The identification of two α laminins has raised the question whether the two versions of laminin trimers found in *Drosophila* act in a redundant fashion or if they might play individual roles during organogenesis and ECM self-assembly. We further addressed this point by analyzing the visceral morphology and basement membrane formation in *wing blister* and *LanA* mutant embryos in comparison to *LanB2*^{knod} and *daughterless-GAL4* (*da-GAL4*) > *UAS-LanB2RNAi* animals as well as double mutants of *LanA* and *wb* (Fig. 3a–f). In *wt* embryos, a sheet of *β*3TUB-positive visceral muscles covers the four-chambered midgut and is

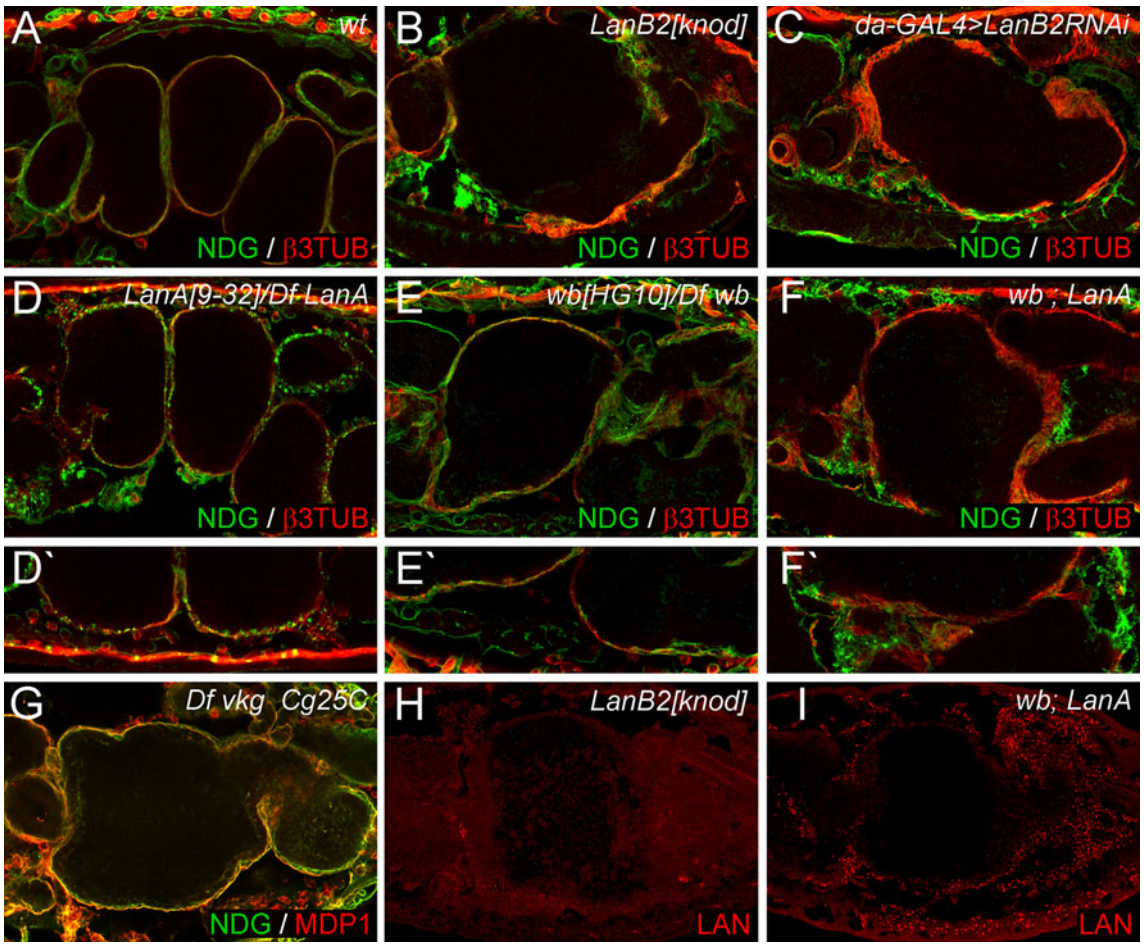

Fig. 3 Different *Laminin* trimers are involved in ECM assembly and midgut morphogenesis. **a** *wt* embryos exhibit a four-chambered midgut covered by a visceral muscle layer and NDG-positive ECM. **b** In *LanB2*^{knod} mutant embryos the NDG-positive ECM is scattered and the midgut displays the characteristic dumpling-shape. **c** *da-GAL4* > *UAS-LanB2RNAi* (*da-GAL4* > *LanB2RNAi*) induced knockdown causes defects in the embryonic midgut and in the ECM that are similar to *LanB2* mutant embryos. (**d**, **d**′) Transheterozygous *LanA*$^{9-32}$*/Df LanA* embryos display normal midgut morphology but a spot-like NDG distribution on the organ surface (**d**′). (**e**, **e**′) *wb*^{HG10}*/Df wb* embryos exhibit a slightly irregular constricted midgut with local adhesion defects (**e**′) of NDG-positive ECM sheets. (**f**, **f**′) Double mutants of *wb*^{HG10}*/Df wb; LanA*$^{9-32}$*/Df LanA* (*wb*; *LanA*) almost phenocopy *LanB2* mutant animals and display disrupted sometimes spotted NDG distribution (**f**′). **g** Embryos deficient for both type IV collagen genes show only minor aberrations in the ECM arrangement. **h**, **i** Laminin signals are absent in *LanB2*^{knod} mutant embryos (**h**) but not in laminin-expressing tissues (particularly the fat body) of *wb*; *LanA* double mutant embryos (**i**) that also exhibit rudimentary laminin signals in or around the midgut

closely associated to the thin nidogen/entactin (NDG)-positive layer of ECM (Fig. 3a). This arrangement is severely disturbed in $LanB2^{knod}$ mutant embryos (Fig. 3b) that exhibit a one-chambered midgut and plaques of ECM that appear loosely attached to the organ surface. Similar defects were also observed due to the RNAi-induced knock down of LanB2 in *da-GAL4 > UASLanB2RNAi* animals (Fig. 3c). Analyzing *LanA* mutant embryos (Fig. 3d), we observed that the midgut has formed properly although *LanA* mutant embryos do not show an early polarization of endodermal midgut cells [24]. In addition, ECM assembly in *LanA* mutant embryos seems to be severely affected. While NDG still associates with the visceral muscles and other tissues, the formation of a thin ECM layer around these structures is impaired and a spot-like distribution of NDG is observed (Fig. 3d′). In accordance to former analysis of *LanA* mutant embryos that display a highly fragmented basement membrane on the ultrastructural level [23], our observations further indicate an important role of *LanA* during ECM self-assembly and BM formation. Also, *wb* mutant embryos have been reported to develop proper midgut morphology [18] and moreover display the formation of continuous NDG-positive ECM sheets that cover all internal organs (Fig. 3e). Upon closer examination, we detected mild defects during midgut chamber formation and at higher magnification we observed local detachment between midgut and surrounding ECM (Fig. 3e′). However, the removal of both laminin α subunits in *wb; LanA* double mutant embryos (wb^{HG10}/*Df wb;* $LanA^{9-32}$/*Df LanA,* Fig. 3f) enhances the visceral defects and the disruptive ECM resembling the phenotype of *LanB2* mutant animals but seems not to reach the strength of the *LanB2* phenotype. Interestingly, the spot-like distribution of NDG, initially observed in *Df LanA* embryos, is still present at most BMs of *wb; LanA* double mutant embryos (Fig. 3f′).

Therefore, we stained *wb; LanA* double mutant embryos in different allelic combinations with antibodies to secreted laminin (LAN) and detected strong signals within the fat body and the hemocytes (Fig. 3i). Since LAN signals are absent in *LamininB2*-deficient (Fig. 2p) and $LanB2^{knod}$ embryos (Fig. 3h) the intracellular signals observed in *wb*; *LanA* double mutants could be explained by stable LanB1/LanB2 heterodimers that form before the incorporation of a laminin α subunit occurs [55]. Our observation that LAN signals are mainly present in tissues that normally express *LanA* and *LanB2* subunits (Fig. 2) further implies a block of laminin secretion in *wb; LanA* animals. In conclusion, our observation that the absence of single laminin trimers causes different phenotypes that are only partially compensated by the remaining trimer indicates that *LamininA* and *wing blister* might act in a cumulative way and at multiple steps during ECM assembly and midgut development rather than triggering one developmental step in complete redundancy.

ECM assembly and basement membrane formation is disturbed in *LanB2* mutant embryos

Our observation that secretion and extracellular deposition of laminin is impaired in $LanB2^{knod}$ has raised the question of how ECM assembly and basement membrane formation takes place in the absence of LanB2. To achieve this, embryos were double-stained with anti-nidogen/entactin (NDG) and anti-macrophage-derived-proteoglycan-1 (MDP1) that recognizes papilin [48, 56]. Since NDG has been shown to interact with the laminin γ subunit [21, 57], it could be utilized to differentiate between molecules of the basement membrane that are directly linked to laminin and other secreted ECM components. In *wt* embryos, NDG and MDP1 cover the surface of internal organs (Fig. 4a–c). While NDG is detected in thin sheets that closely stick to the organ surface (Fig. 4a), MDP1 covers a wider range around the midgut and seems not as closely attached as NDG (Fig. 4b). As a result, NDG and MDP1 are only co-localized in the ECM layer that are directly associated with the midgut surface whereas the distal regions of the basement membrane exhibit the presence of MDP1, solely (Fig. 4c). By analyzing $LanB2^{2}$ mutant embryos we found that the arrangement of NDG and MDP1 was highly disturbed (Fig. 4d–f). NDG is no longer arranged in thin sheets and the overall distribution of MDP1 and NDG appears fringy. In conclusion, a complete overlap of NDG and MDP1 expression is observed throughout the gritted ECM in *LanB2* mutant embryos, most likely indicating the breakdown of the highly ordered basement membrane structure.

It has been assumed that secreted laminins are able to self-assemble to a basal scaffold that is needed for further secretion of other ECM components [58, 59]. To analyze the secretion of ECM components in the absence of *LanB2*, we examined the distribution of the *Drosophila* SPARC protein [60] (Fig. 4j–l). In *wt* embryos, SPARC can be detected in and around the hemocytes and shows a partial overlap with MDP1 expression on the distal surface of the midgut (Fig. 4g–i). In *LanB2* mutant embryos (Fig. 4j–l), SPARC is still expressed in hemocytes and the fat body but secretion and extracellular deposition appears sparsely, indicating that SPARC deposition depends on laminin. Recent analysis of SPARC mutant embryos revealed that collagen IV deposition in the BM is impaired [50]. Therefore, we analyzed the distribution of a type IV collagen encoded by the *viking (vkg)* locus utilizing G454, a GFP protein trap allele of *vkg* (vkg^{G454}). vkg^{G454}/+ embryos develop normally and exhibit strong GFP signals that widely overlap with the MDP1 expression pattern (Fig. 4m–o). In contrast to this, GFP-expression in $LanB2^{knod}$ mutant embryos (vkg^{G454}/+; $LanB2^{knod}$) is strongly reduced around the midgut and the ventral nerve

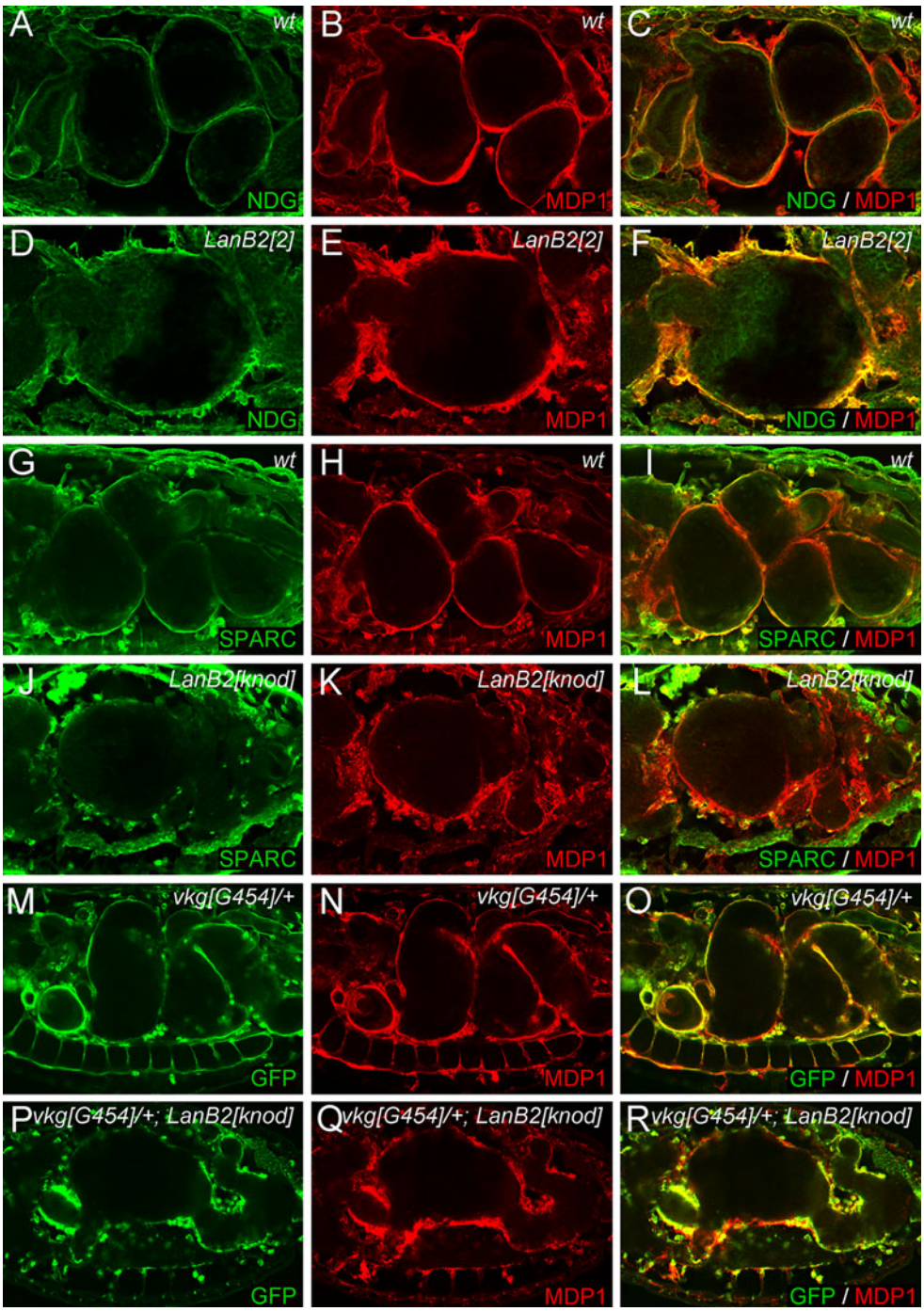

Fig. 4 ECM formation in the absence of *LamininB2*. Confocal sections of stage 16 *wt* and *LanB2* mutant embryos. **a–c** In *wt* embryos NDG is localized in the ECM next to the midgut while MDP1 is also present in distal ECM layers. **d–f** In $LanB2^{2}$ mutant embryos, NDG fails to form thin sheets and is equally distributed within the highly fragmented MDP1-positive ECM. **g–i** SPARC expression is detected on hemocytes and on the visceral basement membrane. **j–l** In $LanB2^{knod}$ mutant embryos SPARC is still expressed in hemocytes but secreted SPARC is almost completely absent in the remaining ECM. **m–o** *VKG::GFP* expression overlaps with MDP1 in vkg^{G454}/+ embryos (**p–r**) and is reduced around the midgut and the ventral nerve cord in vkg^{G454}/+ ; $LanB2^{knod}$ animals

chord while the expression around the proventriculus and the posterior midgut appears blurred (Fig. 4p–r). In addition, the assembly of an initial ECM scaffold seems not much affected in embryos lacking both type IV collagen genes *Cg25C* and *vkg* (*Df vkg Cg25C*, Fig. 3g). Although the MDP1-positive ECM sheets appear thinner than in the *wt* situation, MDP1 and NDG form distinct layers and surround the midgut completely, indicating a negligible

role of type IV collagens during the formation of an initial ECM network. Taken together, the distribution of laminin-associated ECM components and the extracellular deposition of the collagen IV network are severely disturbed in *LanB2* mutants, indicating the importance of an initial laminin meshwork for basement membrane assembly in *Drosophila*.

Visceral development in the absence of *LanB2*

Earlier observations in *wt* embryos revealed the presence of BMs between endodermal cells and the visceral muscles [61]. Our finding that BM assembly is severely disturbed in *LanB2* mutant embryos now raises the question if interactions between the visceral muscles and the endoderm could depend on the formation of a functional BM around visceral tissues. The visceral analysis of *FasIII-GAL4 > UMG* otherwise *wt* embryos at stage 13 reveals that the visceral myotubes stretch, adopt a regular dorso-ventral orientation, and begin to grow out and elongate in the dorsal and ventral directions (Fig. 5a). In contrast to this, a uniform dorso-ventral orientation of visceral myotubes fails in *FasIII-GAL4 > UMG*; $LanB2^{knod}$ mutant embryos (Fig. 5b) although myotube stretching and the formation of filamentous processes (arrows in Fig. 5a, b) can be observed. We also noticed that nidogen-positive BMs have formed at the edges of *wt* visceral muscle strands (Fig. 5c) while only fragmented patches of ECM can be detected in *LanB2* mutant embryos that additionally display a delay in the fusion of the anterior and posterior midgut primordia (AMG and PMG, Fig. 5d, white mark). Interestingly, filamentous actin (F-actin) seems to be concentrated at the contact sites of visceral muscles and the NDG-positive layer in *wt* embryos (Fig. 5e), indicating a potential correlation of ECM distribution and the dorso-ventral stretching of visceral myotubes. This finding is further confirmed since visceral myotubes of *LanB2* mutant embryos (Fig. 5f) stretch out to contact the remaining, randomly distributed NDG-positive patches and accumulate F-actin at the muscle tips that are directly associated with these ECM remnants (arrows in Fig. 5f). Similar results were obtained when we analyzed the distribution of dystroglycan (DG) a potential adhesion receptor of laminin that provides connections to the actin filament network and shows a strong expression in the visceral muscles of *Drosophila* embryos [42]. In *wt* embryos DG is present at the membranes of all visceral myotubes but concentrates at the edges of the visceral bands that completely extend over the midgut endoderm (Fig. 5g). In the absence of *LanB2* (Fig. 5h), DG accumulates at the tips of the randomly aligned visceral myotubes, indicating their capacity to stretch and elongate. Therefore, the formation of highly organized ECM structures like BMs might not be necessary to induce stretching and outgrowth of visceral myotubes but ECM molecules might provide guidance for the visceral myotubes during their dorso-ventral adjustment and during the subsequent myotube stretching.

Interestingly, the loss of *LanB2* also affects the anterior migration process of longitudinal visceral muscles (LVMs). During stage 12, LVMs can be found in close contact to the visceral mesoderm and migrate along the whole range of the circular visceral muscle strands in *croc-lacZ*-expressing embryos (Fig. 5i). The first contact between both muscle primordia is made in *croc-lacZ*; $LanB2^{knod}$ mutant embryos and also maintained during the longitudinal migration process indicating a regular contact of both tissues and moreover proper cell adhesion (Fig. 5j). However, the number of LVMs that reach the anterior margin of the circular visceral muscle strands is reduced and the migrating longitudinal muscle cells exhibit an aberrant shape (Fig. 5j, arrows in n, p). Recent analysis [28] suggests that early association of longitudinal precursor cells with their visceral muscle template occurs at a time when no functional ECM covers the visceral muscle anlagen (Fig. 2d). Therefore, we wished to examine the function of the developing ECM during the migrating process by visualizing the developing visceral ECM with MDP1 in *croc-LacZ* and *croc-LacZ;* $LanB2^{2}$ mutant embryos. In *wt* embryos at stage 12, the migrating longitudinal muscle cells are embedded in ECM probably secreted by the surrounding hemocytes (arrowheads in Fig. 5m). Whereas in *LanB2* mutant embryos, MDP1-expressing hemocytes (arrowheads in Fig. 5n) are nearly indistinguishable from the also MDP1-positive ECM remnants that are found beside the migrating longitudinal muscle cells but do not surround them. Interestingly, we observed an enhanced number of myoblasts between the strands of migrating myoblasts that stretch in dorsoventral orientation thereby crossing the main migration direction (arrow in Fig. 5n, p). After migration differentiated longitudinal myotubes arrange with the ECM into a mesh-like structure (Fig. 5o). In *LanB2* mutant embryos this regular arrangement of longitudinal myotubes is restricted to regions where ECM fragments and hemocytes are concentrated (encircled area in Fig. 5p). Longitudinal muscle precursors which seem not associated with partial ECM display an aberrant morphology and irregular orientation (arrow in Fig. 5p). At the end of embryogenesis, most LVMs observed in *LanB2* mutant embryos appear clumped at those areas of the midgut surface that are also covered with circular muscles (data not shown). Together, these data indicate a role for the ECM for guidance of longitudinal muscle cell migration rather than cell adhesion.

While the elongation of visceral muscles proceeds during stage 13/14, the separation of two rows of visceral nuclei in both halves of the embryo becomes visible in

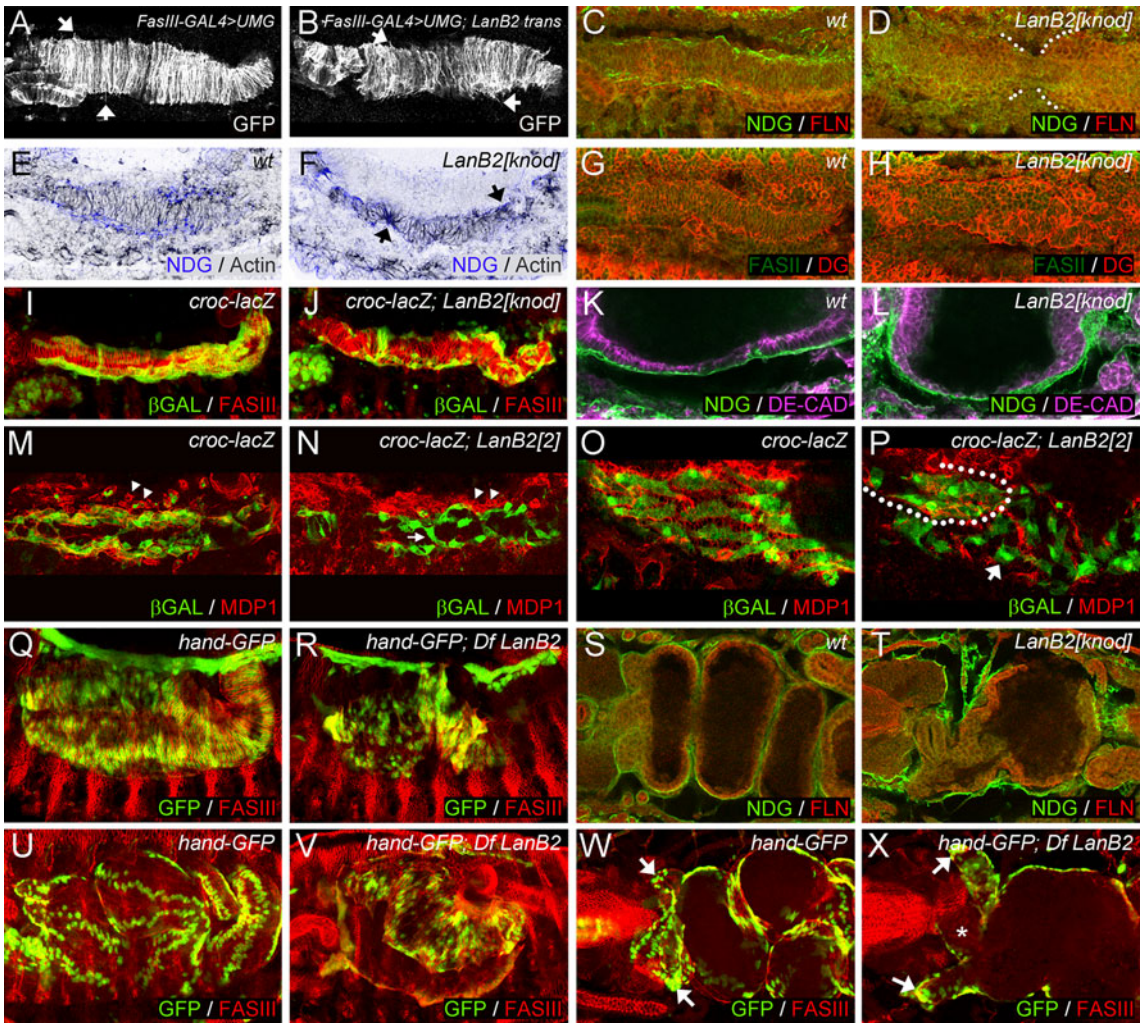

Fig. 5 The role of *LanB2* during visceral muscle differentiation. **a** Dorso-ventral stretching of visceral muscles in stage 13 *FasIII-GAL4 > UMG* embryos. **b** *FasIII-GAL4 > UMG; LanB2* mutant embryos show disordered myotube stretching (*arrows* in **a**, **b** point to filamentous processes). NDG is present in distinct ECM arrays at the edges of the visceral muscles in stage 13 *wt* embryos (**c**) but absent in *LanB2* embryos that also display delayed midgut migration (**d**, *white dots* mark the edges of the midgut endoderm). F-actin (actin, *inverted grey color*) concentrates in visceral muscle tips that contact the ECM (**e**). *LanB2* mutant embryos exhibit apical accumulation of F-actin in visceral myotubes that still stretch towards the remaining ECM fragments (**f**). **g**, **h** Expression of dystroglycan (*DG*) resembles F-actin distribution in *wt* and $LanB2^{knod}$ mutant embryos. Longitudinal muscles migrate along the visceral mesoderm in *croc-lacZ* embryos at stage 12 (**i**) while this migration is reduced in *croc-lacZ;* $LanB2^{knod}$ embryos (**j**). Proper endoderm migration and epithelium formation can be observed in *wt* (**k**) but not in $LanB2^{knod}$ mutant (**l**) embryos. The migrating longitudinal muscles are embedded in MDP1-expressing hemocytes (*arrowheads*) in *croc-lacZ* embryos at stage 12 (**m**) but not in *croc-lacZ;* $LanB2^{knod}$ embryos (**n**) where hemocytes and ECM remnants (*arrowheads*) are mainly found beside the migrating myoblasts (*arrows* in **n**, **p**). **o**, **p** Differentiated longitudinal muscles and MDP1-positive ECM arrange in a mesh-like structure in contrast to *LanB2* mutant embryos where only muscles that contact ECM remnants exhibit proper shape (*encircled* area in **p**). *hand-GFP*-expression indicates proper dorso-ventral elongation of visceral myotubes in *wt* embryos at stage 14/15 (**q**) but irregular distribution of visceral nuclei and impaired elongation in *LanB2* animals (**r**). Nidogen-covered visceral mesoderm attaches closely to the midgut endoderm in *wt* embryos at late stage 15 (**s**), while visceral tissues detach in the absence of *LanB2* (**t**). At the end of embryogenesis visceral nuclei arrange in distinct rows (**u**), whereas the visceral mesoderm of *Df LanB2* embryos (**v**) fails to cover the porous midgut chamber. **w** In *wt* embryos, the gastric caeca (*arrows*) bud in the anterior part of the midgut. **x** In *LanB2* mutant embryos, the gastric caeca (*arrows*) appear rounded and the proventriculus (*asterisk*) shows a defective morphology

hand-GFP embryos (Fig. 5q). We also observed the separation of visceral nuclei in *hand-GFP; Df LanB2* mutant animals (Fig. 5r), indicating again that these muscles are capable to elongate. However, in direct comparison to *hand-GFP* embryos, the distance between the two nuclei of one visceral myotube seems to be shortened. Moreover, small gaps appear in the developing midgut that become only barely covered with visceral myotubes and some visceral muscles start to close ranks, which results in the local accumulation of visceral tissues. At stage 16, visceral

muscles of *LanB2*-deficient embryos (Fig. 5v) are elongated but fail to cover the extended gaps in the midgut chamber that also miss an intact ECM (Fig. 5t). We also noticed that visceral myotubes that had detached from the endoderm at earlier stages now appear clustered and rather undifferentiated. As a result, *LanB2* mutant embryos exhibit the absence of a continuous web of muscles that is typical for *wt* embryos at the same stage (Fig. 5u).

Analyzing endoderm development in *LanB2* mutant embryos, we observed that in addition to the delayed fusion of AMG and PMG (Fig. 5d) most endodermal cells remain their roundish morphology and show no apical concentration of *Drosophila* epithelial cadherin (DE-CAD), indicating that the mesenchymal to epithelial transition fails in *LanB2* mutant embryos (Fig. 5l). Instead of forming a continuous epithelial layer that contacts the NDG-covered visceral muscles in *wt* embryos (Fig. 5k), only few midgut cells have completed their migration process towards the fusion site of AMG and PMG in *LanB2* animals (Fig. 5l) while most endodermal cells remain at the anterior and posterior parts of the prospective gut. This altered distribution of endodermal cells seems to result in the formation of extending gaps within the midgut endoderm that become not enclosed by the NDG-covered visceral muscles (Fig. 5t). *LanB2* mutant animals (Fig. 5t, x) also display aberrations during proventriculus development (Fig. 5x, asterisk) and the gastric caeca appear rounded and fail to elongate properly in comparison to the *wt* situation (arrows in Fig. 5w, x). Taken together, our analyses suggest that *LanB2* seems to be crucial for the proper migration and distribution of endodermal cells along the visceral muscles and the formation of continuous ECM sheets that cover both tissues. Our observation that visceral myotubes of *LanB2* mutant embryos still have the potential to elongate but fail to arrange in a regular dorsoventral orientation and are not able to cover gaps in the midgut endoderm indicates an endoderm dependent step in visceral myogenesis. Therefore, the endodermal cell sheet seems to function as ECM covered substratum that allows proper orientation of stretching visceral muscles and further provides a guidance function for the outgrowth of visceral myotubes.

LanB2 interacts genetically with *thrombospondin* and *kon-tiki*

Beneath the expression of laminin at muscle tendon sites (Fig. 2k, l) we observed a mild somatic muscle phenotype in *LanB2* mutant embryos suggesting a role for laminin in muscle targeting and attachment. Therefore, we performed genetic interaction experiments with *LamininB2* and *thrombospondin* (*tsp*), an ECM protein that is specifically expressed in both developing and mature epidermal tendon cells. The phenotype of *tsp* mutant embryos is characterized by detachment of contracting myotubes from their tendon cells during the hatching process [38]. We observed an overall enhancement of somatic muscle distortions resembled by a disrupted muscle pattern combined with an additional myoblast fusion defect in late-stage *tsp*; *LanB2* double mutant embryos, indicating that these factors interact genetically (Fig. 6g, h).

LanB2 mutant embryos also display defects in the attachment of single ventral-longitudinal (VL) muscles (Fig. 6e, asterisk). The transmembrane protein kon-tiki has been identified as mediator of muscle target site recognition in *Drosophila* and mutant embryos display defects in the attachment of the four VL muscles that exhibit a rounded up morphology (asterisk in Fig. 6c). Therefore, *kon* might be a suitable candidate to mediate laminin derived signals during the process of myotube target site recognition. To study genetic interaction between both genes we analyzed the somatic muscle pattern in kon^{NP7048} and $LanB2^{2}$ mutant animals, in double mutant embryos (kon^{NP7048}; $LanB2^{knod}$) as well as in single mutants with the respective copy of the reciprocal mutation (Fig. 6). As further control we dissected genetic interactions between $LanB2^{knod}$ and *kon*-deficient as well as $LanB2^{knod}$ and kon^{NP7048} embryos (data not shown). In comparison to the *wt* muscle pattern (Fig. 6a) *kon* mutant embryos display attachment defects (Fig. 6c, asterisk) of VL muscles that appear roundish in kon^{NP7048} animals. This phenotype is severely increased in *Df kon* embryos, which additionally exhibit the separation of dorsal muscles from the muscle tendon sites (data not shown). Reducing one copy of *LanB2* does not result in conspicuous effects in the somatic muscle pattern of *kon* mutant embryos (Fig. 6d), while *kon*; *LanB2* double mutant embryos (Fig. 6b) exhibit attachment defects of most ventral muscles and randomly distributed gaps within the dorsal and lateral muscle groups. Vice versa, one copy of *kon* in a *LanB2* mutant background (kon^{NP7048}/+; $LanB2^{knod}$) enhances the somatic phenotype of *LanB2* animals. These embryos exhibit more gaps in their overall muscle pattern and show an increased amount of unfused myoblasts (arrows) and not attached myotubes (Fig. 6f). A similar, slightly enhanced effect was observed in *Df kon*/+ ; $LanB2^{knod}$ embryos (data not shown), that probably relies on the stronger somatic phenotype already observed in *Df kon* and *Df kon*; $LanB2^{knod}$ double mutant embryos.

Discussion

The role of laminin during organogenesis

In *Drosophila*, four genes have been identified that encode for laminin subunits most likely resulting in the formation

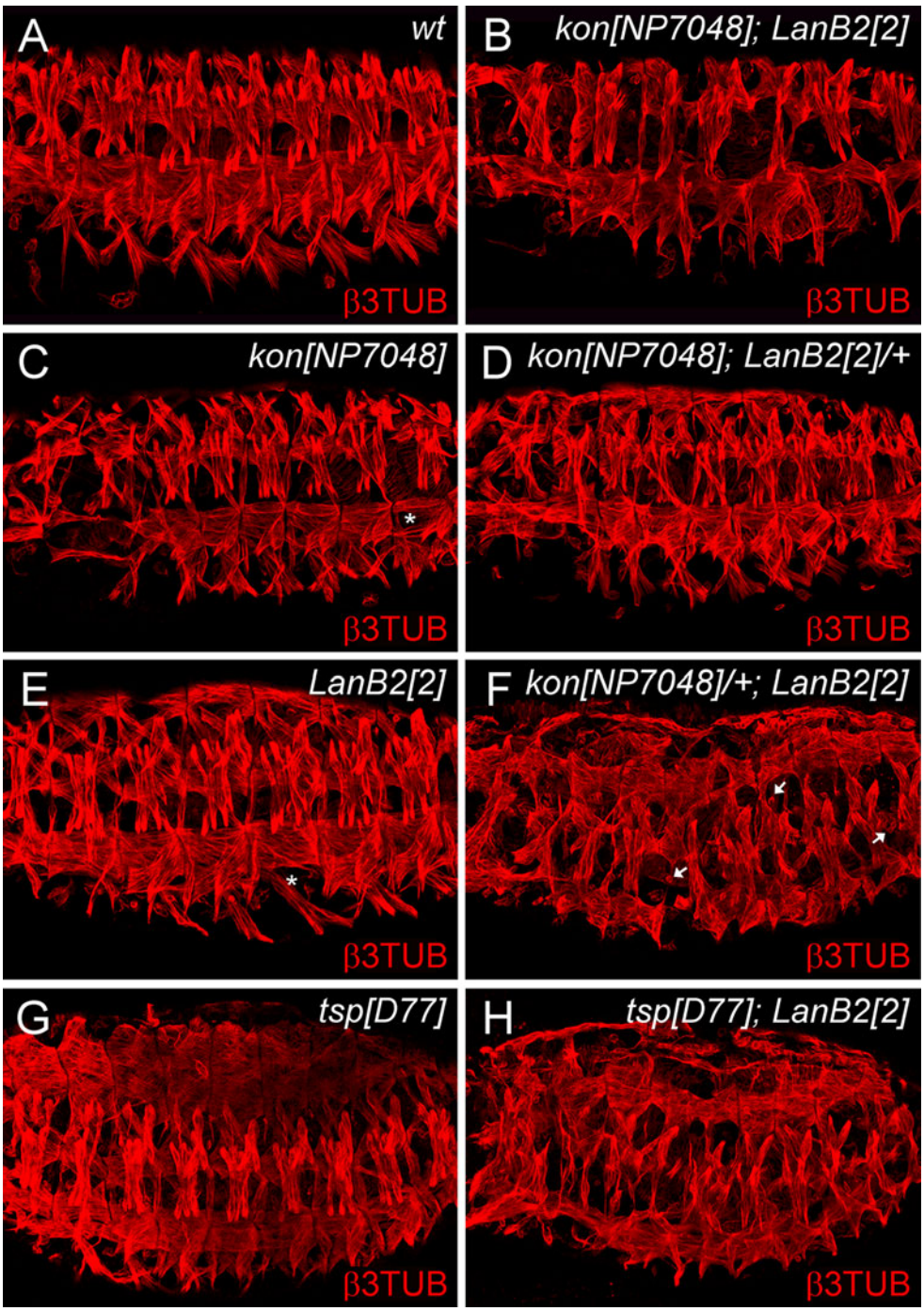

Fig. 6 *LanB2* interacts genetically with *kon-tiki* and *thrombospondin.* The somatic muscles of stage 16 embryos were examined with antibodies to *β*3-tubulin (*β*3TUB). **a** Muscle pattern of *wt* embryos. **b** In *LanB2*; *kon* double-mutants the ventro-lateral muscle groups exhibit severe attachment defects, whereas the dorsal musculature display several gaps and unfused myoblasts. **c** kon^{NP7048} mutant embryos display detached single ventral-longitudinal muscles (*asterisk*). **d** Reducing one copy of *LanB2* in *kon* mutant embryos leads to a similar somatic phenotype than that observed in embryos mutant for *kon* solely. **e** *LanB2* mutant embryos exhibit randomly distributed gaps and some missing or not attached single muscles (*asterisk*). **f** The reduction of one copy *kon* in *LanB2* mutant embryos strongly enhances the appearance of gaps in the ventral and dorsal muscle groups and unfused myoblasts (*arrows*). **g** The $thrombospondin^{D77}$ (tsp^{D77}) phenotype exhibits partially disorganized dorsal muscles and some filamentous processes. This mild muscle phenotype becomes drastically enhanced by muscle movements during the hatching process (not shown). **h** Strong enhancement of somatic muscle defects is found in unhatched tsp^{D77}; $LanB2^{2}$ double mutants

of two different heterotrimers [18–20, 47, 62, 63]. Our finding that the extracellular deposition of laminin trimers fails in *LanB2* mutant embryos supports this model of only two laminin heterotrimers in *Drosophila*, each consisting of a LanB1/LanB2 core unit and either the LanA or Wb chain. Interestingly, the prominent midgut defect that led to the identification of the *knödel* allele is only observed in *LanB2* and *LanB1* mutant animals while defects in the heart, somatic muscles, and other tissues are present in mutations of every laminin subunit [18, 24, 25]. Our analyses reveal that this midgut phenotype primarily relies on the improper migration of endodermal midgut cells and the loss of their epithelial polarity, which interferes with the formation of a coherent endoderm sheet and finally impairs the adhesion between visceral tissues.

Visceral muscle differentiation is not generally inhibited in *LanB2* mutant embryos but is severely reduced in midgut regions where gaps appear in the endodermal layer. This is also supported by our recent observations on *huckebein* (*hkb*) mutant embryos that display a complete block in late visceral muscle differentiation in the absence of endodermal cells [28]. Since PS integrin mutant embryos have been reported to exhibit defective migration of primordial midgut cells as well and, moreover, display shades of visceral phenotypes that resemble the midgut defects that we observed in both *hkb* and *LanB2*, it seems likely that coordinate interactions between laminin and integrin receptors are essential for the proper organization and arrangement of visceral tissues [12, 64, 65]. Laminin also affects the direction and velocity of neurite outgrowth in cell culture and in vivo [66]. These findings turn out to be surprisingly reminiscent of our observations that a directed orientation of circular visceral myotubes fails and the subsequent outgrowth was delayed in *LanB2* mutant embryos that moreover display irregular-shaped and mislocalized LVMs indicating a role for visceral ECM for guidance of these muscles.

Genetic interactions with *LamininB2*

Our data suggests a genetic interaction between *kon-tiki* and *Laminin* during somatic muscle targeting and attachment. The transmembrane protein kon-tiki shares great homology with the vertebrate NG2/CSPG4 family proteins but lacks a characteristic chondroitin sulphate modification [39, 40]. Interestingly, chondroitinase treated NG2 is capable of binding laminin in vitro [67], suggesting a similar scenario for the genetic interaction between *LanB2* and *kon* during *Drosophila* somatic myogenesis. On the other hand, Tillet et al. [68] reported that NG2 transfected cells fail to migrate on laminin-coated surfaces, indicating an indirect nature for the observed genetic interaction. Estrada et al. [39] revealed a genetic interaction between *kon* and the αPS1 encoding gene *multiple endogenous wings* (*mew*) in an RNAi-based approach. Since LanA is also a potential ligand for PS1 integrin in *Drosophila* [69], it remains elusive whether laminin or PS1 integrin interact directly with Kon or whether binding between laminins and integrins plays a permissive role for Kon signaling during *Drosophila* myogenesis.

While laminin seems to be broadly expressed within the ECM, the deposition of other matrix molecules appears restricted, indicating local variations in ECM composition. The glycoprotein thrombospondin (Tsp) is only expressed in the tendon cell matrix and has been reported to bind laminin in vitro [38, 70, 71]. Interestingly, the phenotypic enhancement observed in *LanB2*; *tsp* double mutant embryos appears also clearly in dorsal muscle groups that are otherwise less affected in *tsp* mutant embryos. Therefore, it seems possible that local variations in the ECM composition can partially modulate the loss of laminin, resulting in differently pronounced phenotypes.

The role of laminin for ECM assembly and basement membrane structure

The ability of laminin trimers to spontaneously self-assemble into polymeric networks and the various interactions observed between these multidomain proteins and other ECM components has outlined the central role of laminin during ECM self-assembly and basement membrane (BM) formation [52, 58, 72]. A current model proposes the existence of laminin and collagen IV-associated networks within BMs that are cross linked via nidogen (NDG) and other ECM molecules [21, 73]. Our observation, that NDG forms a discrete layer within MDP1-positive BM and that this layer disperses in *LanB2* mutant embryos supports the conception of different ECM networks within BMs. Based on the analysis of embryoid bodies derived from embryonic stem cells, Li et al. [74] revealed the existence of a basal laminin scaffold that serves as substratum for further deposition of ECM molecules into BMs. The decrease of collagen IV and SPARC in *LanB2* mutant embryos strengthens the assumption of a hierarchy in BM assembly and further indicates the importance of a basal laminin scaffold for the structural properties of BMs and their capacity to modulate cell functions.

The analyses on ECM formation in the absence of both laminin heterotrimers, reflected by the loss of either *LanB1* [25] or *LanB2* (this work), unveiled a breakdown of BM organization while *LanA*-deficient animals display frequently fragmented BMs and the loss of *wb* results in a mild BM adhesion defect. Detailed ultrastructural analyses of *LanA* mutant embryos revealed the presence of fragmented BMs that are partially attached to the cell surface

[23]. Therefore, the LanB1/LanB2/LanA trimer has unique functions during laminin polymerization and ECM self-assembly while the LanB1/LanB2/Wb heterotrimer could play a redundant role, potentially anchoring cellular receptors to the ECM. However, our analysis of *wb*; *LanA* double mutant embryos additionally suggests a maternal component of laminin, since the ECM morphology observed in these embryos partially resembles the weaker defects of *LanA*-deficient embryos but not the BM disruption level of *LanB1* or *LanB2* mutant animals. A maternal component has been suggested previously for *wb* and also *LanA* [18, 75]. This would support the idea that formation of LanB1/LanB2 dimers initiates preliminary laminin trimerization in the presence of maternal laminin α subunits that could otherwise function as single subunits during early embryogenesis.

Recently, a model for the formation of a polygonal meshwork of laminin, transmembrane receptors, and cytoskeletal components, which is driven by the synergistic interactions between laminins and between laminin and cellular receptors, has been proposed [76, 77]. Our observation that visceral myotubes are still capable to differentiate in the absence of LanB2 and moreover display the localization of DG and cortical actin towards their ECM contact sites, indicates a laminin-independent mechanism of DG and actin organization during *Drosophila* visceral myogenesis. This is conformed by the proper distribution of integrins and DG at the muscle attachment sites that has been reported in the absence of *LanB1* [25]. Since *Drosophila* perlecan is capable to bind and localize DG [78], it is conceivable that other ECM components than laminins might be able to recruit and localize receptors and cytoskeletal components during embryonic myogenesis.

Acknowledgments We are grateful to Christian Klämbt for sharing fly stock collections and Susanne Önel for critical reading of the manuscript. We thank Stefan Baumgartner, BDGP, the Bloomington Stock Center, Lynn Cooley, the DGRC, the Developmental Studies Hybridoma Bank, Liselotte Fessler, Michael Hortsch, Elisabeth Knust, Achim Paululat, Renate Renkawitz-Pohl, Rolf Reuter, Maurice Ringuette, John Roote, Martina Schneider, the VDRC, Talila Volk, and Gerd Vorbrüggen for sending materials and fly stocks. This work was supported by the Deutsche Forschungsgemeinschaft to Anne Holz (Ho-2559/3-2 and 3-3).

References

1. Azpiazu N, Frasch M (1993) *tinman* and *bagpipe*: two homeo box genes that determine cell fates in the dorsal mesoderm of *Drosophila*. Genes Dev 7(7B):1325–1340
2. Bate M (1993) The mesoderm and its derivatives. In: Bate M, Martinez Arias A (eds) The development of *Drosophila melanogaster*, vol II. Cold Spring Harbor Laboratory Press, Cold Spring Harbor, New York
3. Campos-Ortega JA, Hartenstein V (1985) The embryonic development of *Drosophila melanogaster*, 1st edn. Springer, Berlin Heidelberg New York
4. Klapper R, Stute C, Schomaker O, Strasser T, Janning W, Renkawitz-Pohl R, Holz A (2002) The formation of syncytia within the visceral musculature of the *Drosophila* midgut is dependent on *duf*, *sns* and *mbc*. Mech Dev 110(1–2):85–96
5. Kusch T, Reuter R (1999) Functions for *Drosophila brachyenteron* and *forkhead* in mesoderm specification and cell signalling. Development 126(18):3991–4003
6. Poulson DF (1950) Histogenesis, organogenesis, and differentiation in the embryo of *Drosophila melanogaster* Meigen. In: Demerec M (ed) Biology of *Drosophila*. Hafner, New York, pp 168–274 (reprinted 1965)
7. Reuter R, Grunewald B, Leptin M (1993) A role for the mesoderm in endodermal migration and morphogenesis in *Drosophila*. Development 119(4):1135–1145
8. San Martin B, Ruiz-Gomez M, Landgraf M, Bate M (2001) A distinct set of founders and fusion-competent myoblasts make visceral muscles in the *Drosophila* embryo. Development 128(17):3331–3338
9. Schröter RH, Buttgereit D, Beck L, Holz A, Renkawitz-Pohl R (2006) Blown fuse regulates stretching and outgrowth but not myoblast fusion of the circular visceral muscles in *Drosophila*. Differentiation 74(9–10):608–621
10. Tepass U, Hartenstein V (1994) Epithelium formation in the *Drosophila* midgut depends on the interaction of endoderm and mesoderm. Development 120(3):579–590
11. Zaffran S, Küchler A, Lee HH, Frasch M (2001) *biniou* (FoxF), a central component in a regulatory network controlling visceral mesoderm development and midgut morphogenesis in *Drosophila*. Genes Dev 15(21):2900–2915
12. Martin-Bermudo MD, Alvarez-Garcia I, Brown NH (1999) Migration of the *Drosophila* primordial midgut cells requires coordination of diverse PS integrin functions. Development 126(22):5161–5169
13. Hynes RO (1992) Integrins: versatility, modulation, and signaling in cell adhesion. Cell 69(1):11–25
14. Hynes RO (2002) Integrins: bidirectional, allosteric signaling machines. Cell 110(6):673–687
15. Aumailley M, Smyth N (1998) The role of laminins in basement membrane function. J Anat 193(1):1–21
16. Durbeej M (2009) Laminins. Cell Tissue Res 339(1):259–268
17. Timpl R (1996) Macromolecular organization of basement membranes. Curr Opin Cell Biol 8(5):618–624
18. Martin D, Zusman S, Li X, Williams EL, Khare N, DaRocha S, Chiquet-Ehrismann R, Baumgartner S (1999) *wing blister*, A new *Drosophila* Laminin α chain required for cell adhesion and migration during embryonic and imaginal development. J Cell Biol 145(1):191–201. doi:10.1083/jcb.145.1.191
19. Montell DJ, Goodman CS (1988) *Drosophila* substrate adhesion molecule: sequence of laminin B1 chain reveals domains of homology with mouse. Cell 53(3):463–473
20. Montell DJ, Goodman CS (1989) *Drosophila* Laminin: sequence of B2 subunit and expression of all three subunits during embryogenesis. J Cell Biol 109(5):2441–2453. doi:10.1083/jcb.109.5.2441
21. Timpl R, Brown JC (1996) Supramolecular assembly of basement membranes. BioEssays 18(2):123–132
22. Henchcliffe C, Garcia-Alonso L, Tang J, Goodman CS (1993) Genetic analysis of laminin A reveals diverse functions during morphogenesis in *Drosophila*. Development 118(2):325–337
23. Prokop A, Martin-Bermudo MD, Bate M, Brown NH (1998) Absence of PS integrins or laminin A affects extracellular adhesion, but not intracellular assembly, of hemiadherens and

neuromuscular junctions in *Drosophila* embryos. Dev Biol 196(1):58–76
24. Yarnitzky T, Volk T (1995) Laminin is required for heart, somatic muscles, and gut development in the *Drosophila* embryo. Dev Biol 169(2):609–618
25. Urbano JM, Torgler CN, Molnar C, Tepass U, Lopez-Varea A, Brown NH, de Celis JF, Martin-Bermudo MD (2009) *Drosophila* laminins act as key regulators of basement membrane assembly and morphogenesis. Development 136(24):4165–4176. doi: 10.1242/dev.044263
26. Hummel T, Schimmelpfeng K, Klämbt C (1999) Commissure formation in the embryonic CNS of *Drosophila*. Development 126(4):771–779
27. Hummel T, Schimmelpfeng K, Klämbt C (1999) Commissure formation in the embryonic CNS of *Drosophila*: I. identification of the required gene functions. Dev Biol 209(2):381–398
28. Wolfstetter G, Shirinian M, Stute C, Grabbe C, Hummel T, Baumgartner S, Palmer RH, Holz A (2009) Fusion of circular and longitudinal muscles in *Drosophila* is independent of the endoderm but further visceral muscle differentiation requires a close contact between mesoderm and endoderm. Mech Dev 126(8–9):721–736
29. Leicht BG, Bonner JJ (1988) Genetic analysis of chromosomal region 67A-D of *Drosophila melanogaster*. Genetics 119(3):579–593
30. Ashburner M, Tsubota S, Woodruff RC (1982) The genetics of a small chromosome region of *Drosophila melanogaster* containing the structural gene for alcohol dehydrogenase. Genetics 102:401–420
31. Woodruff RC, Ashburner M (1979) The genetics of a small autosomal region of *Drosophila melanogaster* containing the structural gene for alcohol dehydrogenase. Genetics 92:133–149
32. Sellin J, Albrecht S, Kölsch V, Paululat A (2006) Dynamics of heart differentiation, visualized utilizing heart enhancer elements of the *Drosophila melanogaster* bHLH transcription factor Hand. Gene Expr Patterns 6(4):360–375
33. Häcker U, Kaufmann E, Hartmann C, Jürgens G, Knochel W, Jäckle H (1995) The *Drosophila* fork head domain protein *crocodile* is required for the establishment of head structures. Embo J 14(21):5306–5317
34. Morin X, Daneman R, Zavortink M, Chia W (2001) A protein trap strategy to detect GFP-tagged proteins expressed from their endogenous loci in *Drosophila*. Proc Natl Acad Sci USA 98(26):15050–15055
35. Wodarz A, Hinz U, Engelbert M, Knust E (1995) Expression of crumbs confers apical character on plasma membrane domains of ectodermal epithelia of *Drosophila*. Cell 82(1):67–76
36. Dietzl G, Chen D, Schnorrer F, Su KC, Barinova Y, Fellner M, Gasser B, Kinsey K, Oppel S, Scheiblauer S, Couto A, Marra V, Keleman K, Dickson BJ (2007) A genome-wide transgenic RNAi library for conditional gene inactivation in *Drosophila*. Nature 448(7150):151–156
37. Chihara T, Kato K, Taniguchi M, Ng J, Hayashi S (2003) Rac promotes epithelial cell rearrangement during tracheal tubulogenesis in *Drosophila*. Development 130(7):1419–1428. doi: 10.1242/dev.00361
38. Chanana B, Graf R, Koledachkina T, Pflanz R, Vorbrüggen G (2007) αPS2 integrin-mediated muscle attachment in *Drosophila* requires the ECM protein thrombospondin. Mech Dev 124(6):463–475
39. Estrada B, Gisselbrecht SS, Michelson AM (2007) The transmembrane protein Perdido interacts with grip and integrins to mediate myotube projection and attachment in the *Drosophila* embryo. Development 134(24):4469–4478
40. Schnorrer F, Kalchhauser I, Dickson BJ (2007) The transmembrane protein Kon-tiki couples to Dgrip to mediate myotube targeting in *Drosophila*. Developmental Cell 12(5):751–766
41. Stute C, Schimmelpfeng K, Renkawitz-Pohl R, Palmer RH, Holz A (2004) Myoblast determination in the somatic and visceral mesoderm depends on Notch signalling as well as on *milliways* (*mili*^{Alk}) as receptor for Jeb signalling. Development 131(4):743–754
42. Schneider M, Baumgartner S (2008) Differential expression of Dystroglycan-spliceforms with and without the mucin-like domain during *Drosophila* embryogenesis. Fly 2(1):29–35
43. Oda H, Uemura T, Harada Y, Iwai Y, Takeichi M (1994) A *Drosophila* homolog of cadherin associated with armadillo and essential for embryonic cell-cell adhesion. Dev Biol 165(2): 716–726
44. Grenningloh G, Rehm EJ, Goodman CS (1991) Genetic analysis of growth cone guidance in *Drosophila*: *fasciclin II* functions as a neuronal recognition molecule. Cell 67(1):45–57
45. Patel NH, Snow PM, Goodman CS (1987) Characterization and cloning of *fasciclin III*: a glycoprotein expressed on a subset of neurons and axon pathways in *Drosophila*. Cell 48(6):975–988
46. Sokol NS, Cooley L (1999) *Drosophila* Filamin encoded by the *cheerio* locus is a component of ovarian ring canals. Curr Biol 9(21):1221–1230
47. Kusche-Gullberg M, Garrison K, MacKrell AJ, Fessler LI, Fessler JH (1992) Laminin A chain: expression during *Drosophila* development and genomic sequence. EMBO J 11:4519–4527
48. Hortsch M, Olson A, Fishman S, Soneral SN, Marikar Y, Dong R, Jacobs JR (1998) The expression of MDP-1, a component of *Drosophila* embryonic basement membranes, is modulated by apoptotic cell death. Int J Dev Biol 42(1):33–42
49. Chartier A, Zaffran S, Astier M, Semeriva M, Gratecos D (2002) Pericardin, a *Drosophila* type IV collagen-like protein is involved in the morphogenesis and maintenance of the heart epithelium during dorsal ectoderm closure. Development 129(13):3241–3253
50. Martinek N, Shahab J, Saathoff M, Ringuette M (2008) Haemocyte-derived SPARC is required for collagen-IV-dependent stability of basal laminae in *Drosophila* embryos. J Cell Sci 121(10):1671–1680
51. Leiss D, Hinz U, Gasch A, Mertz R, Renkawitz-Pohl R (1988) Beta 3 tubulin expression characterizes the differentiating mesodermal germ layer during *Drosophila* embryogenesis. Development 104(4):525–531
52. Beck K, Hunter I, Engel J (1990) Structure and function of laminin: anatomy of a multidomain glycoprotein. FASEB J 4(2):148–160
53. Riechmann V, Rehorn KP, Reuter R, Leptin M (1998) The genetic control of the distinction between fat body and gonadal mesoderm in *Drosophila*. Development 125(4):713–723
54. Holz A, Bossinger B, Strasser T, Janning W, Klapper R (2003) The two origins of hemocytes in *Drosophila*. Development 130(20):4955–4962
55. Kumagai C, Kadowaki T, Kitagawa Y (1997) Disulfide-bonding between *Drosophila* laminin and chains is essential for chain to form trimer. FEBS Letters 412(1):211–216
56. Firth LC, Baker NE (2007) Spitz from the retina regulates genes transcribed in the second mitotic wave, peripodial epithelium, glia and plasmatocytes of the *Drosophila* eye imaginal disc. Dev Biol 307(2):521–538
57. Mayer U, Nischt R, Poschl E, Mann K, Fukuda K, Gerl M, Yamada Y, Timpl R (1993) A single EGF-like motif of laminin is responsible for high affinity nidogen binding. EMBO J 12(5):1879–1885

58. Hamill KJ, Kligys K, Hopkinson SB, Jones JCR (2009) Laminin deposition in the extracellular matrix: a complex picture emerges. J Cell Sci 122(24):4409–4417. doi:10.1242/jcs.041095
59. Yurchenco PD, Amenta PS, Patton BL (2004) Basement membrane assembly, stability and activities observed through a developmental lens. Matrix Biol 22(7):521–538
60. Martinek N, Zou R, Berg M, Sodek J, Ringuette M (2002) Evolutionary conservation and association of SPARC with the basal lamina in *Drosophila*. Dev Genes Evol 212(3):124–133
61. Goldstein MA, Burdette WJ (1971) Striated visceral muscle of *Drosophila melanogaster*. J Morphol 134(3):315–334
62. Chi HC, Hui CF (1988) cDNA and amino acid sequences of *Drosophila* laminin B2 chain. Nucleic Acids Res 16:7205–7206
63. Chi HC, Hui CF (1989) Primary structure of the *Drosophila* laminin B2 chain and comparison with human, mouse, and *Drosophila* laminin B1 and B2 chains. J Biol Chem 264(3):1543–1550
64. Devenport D, Brown NH (2004) Morphogenesis in the absence of integrins: mutation of both *Drosophila* beta subunits prevents midgut migration. Development 131(21):5405–5415
65. Roote CE, Zusman S (1995) Functions for PS integrins in tissue adhesion, migration, and shape changes during early embryonic development in *Drosophila*. Dev Biol 169(1):322–336
66. Luckenbill-Edds L (1997) Laminin and the mechanism of neuronal outgrowth. Brain Res Rev 23(1–2):1–27
67. Burg MA, Tillet E, Timpl R, Stallcup WB (1996) Binding of the NG2 proteoglycan to type VI collagen and other extracellular matrix molecules. J Biol Chem 271(42):26110–26116. doi:10.1074/jbc.271.42.26110
68. Tillet E, Gential B, Garrone R, Stallcup WB (2002) NG2 proteoglycan mediates β1 integrin-independent cell adhesion and spreading on collagen VI. J Cell Biochem 86(4):726–736
69. Gotwals PJ, Fessler LI, Wehrli M, Hynes RO (1994) *Drosophila* PS1 integrin is a laminin receptor and differs in ligand specificity from PS2. Proc Natl Acad Sci USA 91(24):11447–11451
70. Mumby SM, Raugi GJ, Bornstein P (1984) Interactions of thrombospondin with extracellular matrix proteins: selective binding to type V collagen. J Cell Biol 98(2):646–652. doi:10.1083/jcb.98.2.646
71. Subramanian A, Wayburn B, Bunch T, Volk T (2007) Thrombospondin-mediated adhesion is essential for the formation of the myotendinous junction in *Drosophila*. Development 134(7):1269–1278
72. Sasaki T, Fässler R, Hohenester E (2004) Laminin. J Cell Biol 164(7):959–963. doi:10.1083/jcb.200401058
73. Yurchenco PD, Cheng YS, Colognato H (1992) Laminin forms an independent network in basement membranes. J Cell Biol 117(5):1119–1133. doi:10.1083/jcb.117.5.1119
74. Li S, Harrison D, Carbonetto S, Fässler R, Smyth N, Edgar D, Yurchenco PD (2002) Matrix assembly, regulation, and survival functions of laminin and its receptors in embryonic stem cell differentiation. J Cell Biol 157(7):1279–1290. doi:10.1083/jcb.200203073
75. Schöck F, Perrimon N (2003) Retraction of the *Drosophila* germ band requires cell-matrix interaction. Genes Dev 17(5):597–602
76. Colognato H, Winkelmann DA, Yurchenco PD (1999) Laminin polymerization induces a receptor-cytoskeleton network. J Cell Biol 145(3):619–631. doi:10.1083/jcb.145.3.619
77. Colognato H, Yurchenco PD (2000) Form and function: the laminin family of heterotrimers. Dev Dyn 218(2):213–234
78. Schneider M, Khalil AA, Poulton J, Castillejo-Lopez C, Egger-Adam D, Wodarz A, Deng WM, Baumgartner S (2006) Perlecan and dystroglycan act at the basal side of the *Drosophila* follicular epithelium to maintain epithelial organization. Development 133(19):3805–3815